THE
AUSTRALIAN
NATIONAL
UNIVERSITY

RESEARCH SCHOOL OF PHYSICAL SCIENCES

ANU-P/915
March 1985

MAGNETIC MOMENTS, E3 TRANSITIONS AND THE STRUCTURE OF HIGH SPIN CORE EXCITED STATES IN ^{211}Rn

A.R. Poletti, G.D. Dracoulis, A.P. Byrne,
A.E. Stuchbery, S.J. Poletti and J. Gerl

Department of Nuclear Physics, ANU

and

P.M. Lewis

Department of Physics, University of Auckland

INSTITUTE OF ADVANCED STUDIES

ANU-P/915
March 1985

Accepted for publication in Physics Letters B

MAGNETIC MOMENTS, E3 TRANSITIONS AND THE STRUCTURE OF HIGH SPIN CORE EXCITED STATES IN ^{211}Rn

A.R. Poletti[*], G.D. Dracoulis, A.P. Byrne,
A.E. Stuchbery[†], S.J. Poletti and J. Gerl

Department of Nuclear Physics, Research School
of Physical Sciences, Australian National University,
GPO Box 4, Canberra, ACT 2601, Australia.

and

P.M. Lewis

Department of Physics, University of Auckland,
Private Bag, Auckland, New Zealand.

Abstract: The results of g-factor measurements of high spin states in ^{211}Rn are: $E_x=8856+\Delta'$ keV ($J^\pi=63/2^-$), $g=0.626(7)$; $6101+\Delta'$ keV ($49/2^+$), 0.766(8); $5247+\Delta'$ keV ($43/2^-$), 0.74(2); $3927+\Delta$ keV ($35/2^+$), 1.017(12); $1578+\Delta$ keV ($17/2^-$), 0.912(9). These results together with measured E3 transition strengths and shell model calculations are used to assign configurations to the core excited states in ^{211}Rn. Mixed configurations are required to explain the g-factors and enhanced E3 strengths simultaneously.

---

[*] Permanent Address: Department of Physics, University of Auckland, Private Bag, Auckland, New Zealand.

[†] Joint appointment with School of Physics, University of Melbourne, Parkville 3052, Victoria, Australia.

Core-excited isomers of high spin ($J \sim 30\hbar$) were first identified in ^{212}Rn [1], which has four protons outside the doubly closed shell nucleus ^{208}Pb. The yrast states of the neighbouring radon isotopes ^{210}Rn [2] and ^{211}Rn [3,4] have since been identified to comparable spins and there is spectroscopic evidence that core-excited states enter the yrast sequence at excitation energies of 5-6 MeV, similar to the situation in ^{212}Rn. Several different configurations within the shell model [1] and deformed independent particle models [5,7] have been suggested for the highest states in ^{212}Rn, (see also the review by de Voigt et al. [8]); these reproduce the measured magnetic moments. However, as has been pointed out [3,4,9] some of the accepted configurations do not provide a consistent picture of the other properties, specifically the strong E3 transitions which connect the high spin states. These E3 transitions are a signature of the presence of certain orbitals, and importantly, of a simple relationship between the configurations of the pairs of states which they connect.

To elucidate the structure of the proposed core-excited states in the radon region we have carried out g-factor measurements for isomers in ^{211}Rn (and ^{210}Rn), and have also measured the lifetimes of several short-lived isomers to obtain new E3 strengths. These timing measurements will be reported separately [10].

By considering the measured g-factors together with the E3 transition strengths, and with the results of shell model calculations which treat the residual interactions explicitly [9], we aim to identify, or at least restrict, the configuration of the core excited isomers in ^{211}Rn. One surprising conclusion is that a simultaneous description of the static and transition moments requires mixing between the several alternative configurations for each of the highest spin states observed. This result is supported by the calculations which show that the alternative configurations for a given spin may lead to states which lie close in energy.

The new measurements for ^{211}Rn have also necessitated a change in the level scheme from that previously reported.

The g-factors in ^{211}Rn were measured using the TDPAD technique with a pulsed beam of width ∿1 ns, and a 2160 ns separation, from the ANU 14UD Pelletron accelerator. An external magnetic field of 2.42(2)T was applied at right angles to the beam-detector plane, and the Larmor precession was deduced from the spin-rotation patterns obtained with two hyperpure Ge detectors placed at 135° and -135° to the beam axis. High spin states in ^{211}Rn were populated using the ^{204}Hg(^{12}C,5n) reaction at 85 MeV, with a thick liquid mercury target, enriched to 93% in ^{204}Hg. For each detector, the γ-ray energy, and time with respect to the beam pulse were recorded in event-by-event mode. To reduce the data rates, events occurring within a 20 ns window about the beam pulse were filtered out using a fast-veto system.

The spin rotation patterns for the two highest-lying isomers are shown in figure 1. The solid lines are fits to the ratio function using the multi-level formalism given by Häusser et al.[11]. The g-factor and lifetime results for these and lower isomers are summarised in table 1.

The g-factors obtained for the $17/2^-$ and $35/2^+$ isomers given in table 1 are in good agreement with those calculated using additivity and the previously assigned configurations. However, the measured g-factor of +0.74(2) for the 20 ns isomer, an isomer previously attributed to the decay of a $41/2^-$ yrast state [3], disagrees strongly with g=+1.11, expected for the assigned $\{(\pi h^2_{9/2} i^2_{13/2})_{20^+} \otimes \nu p^{-1}_{1/2}\}_{41/2^-}$ configuration. This discrepancy supports the suggestion by Blomqvist [12] that the isomeric lifetime is predominantly due to a core-excited $43/2^-$ state calculated to lie close in energy to the expected yrast $41/2^-$ state. (The g-factor of the related 20^+ yrast state in ^{210}Rn does agree with the $\pi(h^2_{9/2} i^2_{13/2})20^+$ configuration [13].) This leads us to reassign the 20 ns lifetime to a $43/2^-$ level at $5247+\Delta'$ keV which decays by a hindered low energy M1 transition of energy $\Delta'-\Delta$ keV to the $41/2^-$ level at $5247+\Delta$ keV. The expected mean life for the $41/2^-$ state is considerably shorter, about 4.3 ns [14]. The core-excited state suggested by Blomqvist has a configuration $\{(\pi h^3_{9/2} i_{13/2})_{17^-} \otimes \nu^{-2} \otimes \nu g_{9/2}\}_{43/2^-}$ whose g-factor would be +0.755, in good agreement with the observed value of +0.74(2).

Compared to the previously published scheme [3,4] insertion of the $43/2^-$ state leads to an increase of $1\hbar$ in spin of all levels above the $5247+\Delta$ keV state, as shown in the abbreviated scheme given in figure 2. The isomers at $8856+\Delta'$ and $6101+\Delta'$ keV are now assigned as $63/2^-$ and $49/2^+$ respectively.

Four of the states above the $43/2^-$ core-excited state are connected by strong E3 transitions (strengths are shown in figure 2) and the g-factors of the $63/2^-$ and $49/2^+$ isomers also suggest neutron core excitations. We now consider the possible configurations of these states with the dual constraints imposed by the measured g-factors and enhanced E3 transitions. The excitation energies of the unperturbed states were calculated using a formalism similar to that described in ref.[9], with residual interactions taken from experiment where available. We have considered all the previously suggested configurations or those implied by suggested configurations for states in ^{212}Rn [1,5-9].

It is inappropriate to present all the details here, but a distillation and the suggested configurations are given in figure 2. Several comments are in order. Firstly, strong E3 transitions can be associated with a <u>single</u> orbit change involving the protons; $\pi i_{13/2} \rightarrow f_{7/2}$, $\pi i_{13/2} \rightarrow h_{9/2}$, or the neutrons; $\nu j_{15/2} \rightarrow g_{9/2}$, or $j_{15/2} \rightarrow i_{11/2}$. The latter transition in each pair involves a spin flip, and is weaker. Secondly, configurations which involve the simultaneous alignment of high spin protons and high spin neutron <u>holes</u> are unfavoured because of the repulsive proton-neutron hole interaction [5,9]. However this interaction is only strongly repulsive for the stretched case, hence some configurations in figure 2 contain the $f_{5/2}^{-1}$ neutron but with less than maximum alignment. Thirdly, the cost in energy in exciting one or two neutrons across the N=126 shell into the high spin neutron orbitals is compensated for by the strongly attractive proton-neutron interaction [9], and this is a large contribution (between -2 and -4 MeV) to the states given in figure 2.

Columns II and III of figure 2 show the calculated energies of the important configurations, and the double arrows depict expected E3 transitions. Column IV shows the calculated g-factors, and E3 transitions (but arbitrary excitation energies since the unperturbed excitation energies cannot be accurately calculated in some cases) with admixed amplitudes as given in column V. The admixtures were chosen to reproduce the g-factors, and we will make further comment on the implied mixing matrix elements below. To summarise the results of figure 2 briefly; nearly equal admixtures of configurations "γ" and "δ" are required to reproduce the g-factor of the $49/2^+$ state. The same admixtures then reproduce the very strong (46 W.u.) E3 transition connecting the $49/2^+$ and $43/2^-$ states through constructive interference between the $\nu j_{15/2} \rightarrow g_{9/2}$ and $\pi i_{13/2} \rightarrow f_{7/2}$ transitions. The $55/2^-$ state is essentially pure, and its 43 W.u. E3 transition to the mixed $49/2^+$ state is also then reproduced. The g-factors and E3 strengths for related states and transitions in ^{210}Rn agree with the present description [13].

The $63/2^-$ and $57/2^+$ states have configurations similar to the $49/2^+$ and $43/2^-$ states, being double core-excitations with $f^{-1}_{5/2}\ i_{11/2}$ neutrons coupled (not in a stretched manner) to the $49/2^+$ and $43/2^-$ states. The configurations are not exactly equivalent because the interaction between the added neutrons and the valence protons means that the component states do not have the same unperturbed separation as in the lower states. With the mixed amplitudes that reproduce the g-factor of the $63/2^-$ state, a strong $63/2^- \rightarrow 57/2^+$ E3 transition is also predicted, although it is stronger than the observed 31 W.u. transition. The agreement here is less satisfactory than for the transitions lower in the scheme, but the uncertainty in the $57/2^+$ wave function is larger because its g-factor is not known.

The two configurations for $63/2^-$ and $57/2^+$ states shown as dashed lines at the top of columns II and III of figure 3 are not considered to contribute. Although the present simple model, which uses empirical energies, places them close to the observed states, the presence of a $g_{9/2}$ and $j_{15/2}$ neutron simultaneously in these configurations will block the octupole correlation which otherwise lowers the energy of the $j_{15/2}$ neutron state from its true single particle value. (That is, the $j_{15/2}$ neutron as written in the configurations of figure 2 represents the empirical $j_{15/2}$ state which contains a large $(3^- \otimes g_{9/2})_{15/2}$ admixture.)

The required mixing, particularly for the $49/2^+$ and $63/2^-$ states is large, and the large matrix elements implied must be justified. A more sophisticated calculation for the $49/2^+$ and $43/2^-$ states, in which the octupole (and double octupole) couplings are treated explictly (giving a 10x10 matrix for this case), has been carried out and this shows [13] that there are large interactions and components which are hidden in the labelling of figure 3. The results for the $49/2^+$ and $43/2^-$ states are in good agreement with experiment.

Admixtures in such high spin states may also be contrary to the naive expectation that high spin yrast states are usually pure, an expectation based on the grounds that there are usually only a few ways of forming them. This expectation is probably well-founded for fully stretched configurations, but the presence of neutron holes (such as the $f^{-1}_{5/2}$ neutron) in conjunction with aligned high spin protons somewhat paradoxically leads to more competition between stretched and non-stretched configurations.

The partial equivalence between the deformed independent particle model (DIPM), and the shell model description using empirical residual interactions has been discussed, and demonstrated [5,9], however the DIPM will not reproduce repulsive proton-neutron-hole interactions [5]. As discussed above, these may be important for determining the likely yrast configurations of multi-core excited isomers in the radon region.

REFERENCES

1] D. Horn, O. Häusser, T. Faestermann, A.B. McDonald, T.K. Alexander, J.R. Beene and C.J. Herrlander, Phys.Rev.Lett. 39(1977)389.

2] A.R. Poletti, G.D. Dracoulis, C. Fahlander and I. Morrison, Nucl.Phys. A380(1982)335.

3] A.R. Poletti, G.D. Dracoulis, C. Fahlander and I. Morrison, Nucl.Phys. A359(1981)180.

4] G.D. Dracoulis, C. Fahlander and A.R. Poletti, Phys.Rev. C24(1981)2386.

5] K. Matsuyanagi, T. Døssing and K. Neergaard, Nucl.Phys. A307(1978)253.

6] C.G. Andersson, G. Hellström, G. Leander, I. Ragnarsson, S. Aberg, J. Krumlinde, S.G. Nilsson and Z. Szymanski, Nucl.Phys. A309(1978)141.

7] J. Dudek, Z. Szymanski and T. Werner, Phys.Rev. C23(1981)920.

8] M.J.A. de Voigt, J. Dudek and Z. Szymanski, Rev.Mod.Phys. 55(1983)949.

9] A.P. Byrne and G.D. Dracoulis, Nucl.Phys. A391(1982)1.

10] A.R. Poletti, G.D. Dracculis, S.J. Poletti, A.E. Stuchbery, A.P. Byrne and J. Gerl, to be published.

11] O. Häusser, T.K. Alexander, J.R. Beene, E.D. Earle, A.B. McDonald, F.C. Khanna and I.S. Towner, Nucl.Phys. A273(1976)253.

12] J. Blomqvist, private communication.

13] S.J. Poletti, G.D. Dracoulis, A.R. Poletti, A.E. Stuchbery, A.P. Byrne and J. Gerl, to be published.

14] This lifetime is deduced by assuming the same E3 strength for the 1320 keV transition as is observed for the 1181 keV $20^+\to17^-$ transition, the related transition in ^{210}Rn [2].

Table 1. g-factors and mean lives in ^{211}Rn.

Level energy (kev)	J^π	τ (ns)	g [a] measured
1578+Δ	$17/2^-$	860(40) [b]	+0.912 (9)
3927+Δ	$35/2^+$	58 (2) [b]	+1.017(12)
5247+Δ	$41/2^-$	5 (2) [c]	
5247+Δ'	$43/2^-$	20 (3) [c,d]	+0.74 (2)
6106+Δ'	$49/2^+$	42 (1) [d,e]	+0.766 (8)
7400+Δ'	$55/2^-$	2.1(5) [f]	
8169+Δ'	$57/2^+$	3.3(3) [f]	
8856+Δ'	$63/2^-$	290(5) [d,g]	+0.622 (7)

a) Corrected for Knight shift and dimagnetic shielding

$g_{corr} = g_{un}[(1+K)(1-\sigma)]^{-1} = 1.0190\ g_{un}$;

$K=0.05\pm.20\times10^{-2}$ for Rn (Hg) $\sigma=1.914\times10^{-2}$.

b) Reference [3].

c) Assuming a $43/2^-$ state close to the previously assigned $41/2^-$ state (see text and ref.[10]).

d) Present work.

e) Decays by two branches 854 keV (E3), 96(1)%; 366 (M2), 4(1)%.

f) Reference [10].

g) Decays by two branches 1299 keV (E3), 85(2)%, 685 (Q), 15(2)%.

FIGURE CAPTIONS

Figure 1 Spin rotation patterns for the 1299 keV γ-ray, which is fed from the 290 ns, $63/2^-$ isomer, and the 854 keV γ-ray, which has components from the $63/2^-$ isomer, and the 41 ns, $49/2^+$ isomer. The function $R(t) = \frac{W(135°,t)-W(-135°,t)}{W(135°,t)+W(-135°,t)}$ The solid line is a multi-level fit.

Figure 2 Schematic indicating the revised level scheme (column I) with E3 strengths contained in brackets. Columns II and III show the calculated energies and g-factors of the high spin core-excited states, and the strong connecting E3 transitions (double arrows). The transition strengths are in Weiskopff Units. Column IV shows the calculated g-factors and E3 strengths for the admixtures given in column V. The Greek symbols refer to the configurations defined in column II and for the protons $h=h_{9/2}$, $f=f_{7/2}$, $i=i_{13/2}$. For the neutrons $p=p_{1/2}$, $f=f_{5/2}$, $i=i_{11/2}$, $g=g_{9/2}$, $j=j_{15/2}$ and ν^{-2} refers to an unspecified pair of neutron holes coupled to spin zero.

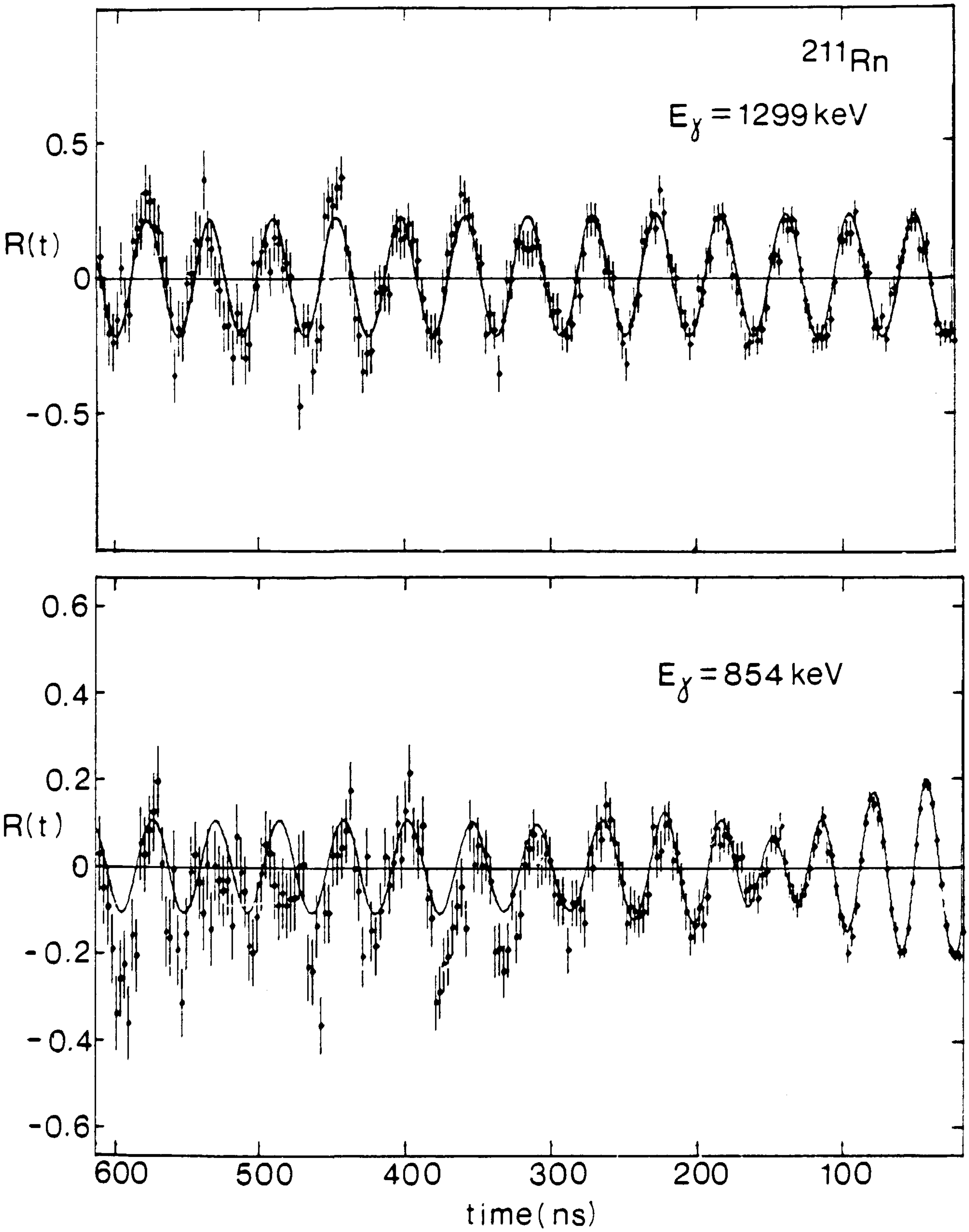
211Rn
Eγ = 1299 keV
0.5
R(t)
0
-0.5
Eγ = 854 keV
0.6
0.4
0.2
R(t)
0
-0.2
-0.4
-0.6
600
500
400
300
200
100
time(ns)

Fig. 1.

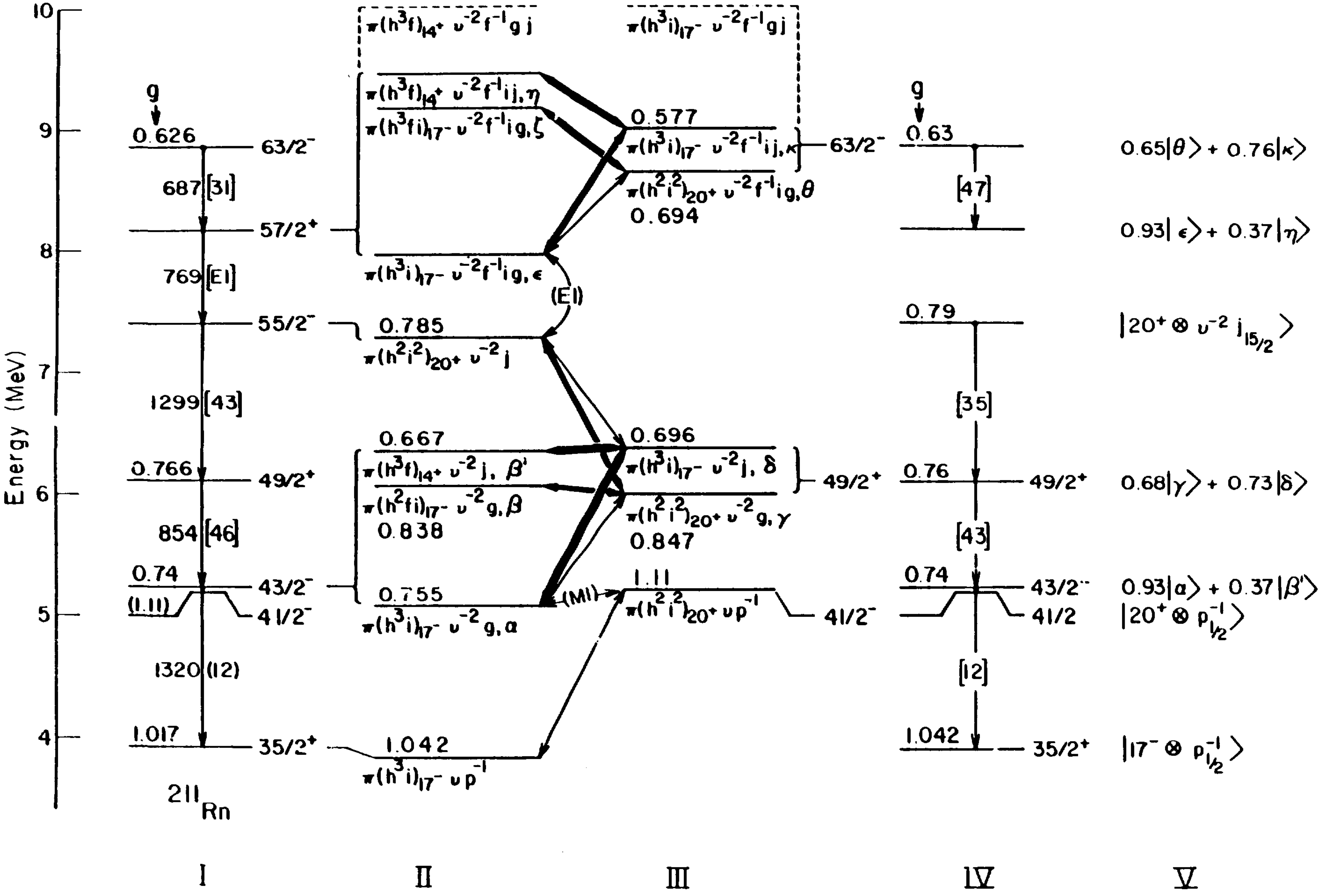
Energy (MeV)
10
9
8
7
6
5
4
g
0.626
63/2⁻
687 [31]
57/2⁺
769 [E1]
55/2⁻
1299 [43]
0.766
49/2⁺
854 [46]
0.74
43/2⁻
(1.11)
41/2⁻
1320 (12)
1.017
35/2⁺
211Rn
π(h3f)14+ ν-2f-1gj
π(h3f)14+ ν-2f-1ij, η
π(h3fi)17- ν-2f-1ig, ζ
π(h3i)17- ν-2f-1ig, ε
(E1)
0.785
π(h2i2)20+ ν-2j
0.667
π(h3f)14+ ν-2j, β'
π(h2fi)17- ν-2g, β
0.838
0.755
π(h3i)17- ν-2g, α
(M1)
1.042
π(h3i)17- νp-1
π(h3i)17- ν-2f-1gj
0.577
π(h3i)17- ν-2f-1ij, κ
π(h2i2)20+ ν-2f-1ig, θ
0.694
63/2⁻
0.696
π(h3i)17- ν-2j, δ
π(h2i2)20+ ν-2g, γ
0.847
49/2⁺
1.11
π(h2i2)20+ νp-1
41/2⁻
g
0.63
[47]
0.79
[35]
0.76
49/2⁺
[43]
0.74
43/2⁻
41/2
[12]
1.042
35/2⁺
0.65|θ⟩ + 0.76|κ⟩
0.93|ε⟩ + 0.37|η⟩
|20⁺ ⊗ ν⁻² j15/2⟩
0.68|γ⟩ + 0.73|δ⟩
0.93|α⟩ + 0.37|β'⟩
|20⁺ ⊗ p1/2⁻¹⟩
|17⁻ ⊗ p1/2⁻¹⟩
I
II
III
IV
V

Fig. 2.